

Physics of Spin Casting Dilute Solutions

Stefan Karpitschka,* Constans M. Weber, and Hans Riegler

Max-Planck-Institut für Kolloid- und Grenzflächenforschung, Potsdam-Golm, Germany

(Dated: December 3, 2024)

We analyze the spin casting of dilute (ideal) binary mixtures of non-volatile solutes in volatile solvents. The system-specific fundamental length and time scales of the process are introduced and an analytical description of the thinning of a volatile liquid film simultaneously subject to spinning and evaporation is presented for the first time. This reveals spin casting essentially as evaporative thinning of a hydrodynamically flattened film. The spatio-temporal composition evolution within the thinning film is analyzed. We identify the Sherwood Number as fundamental process parameter characterizing whether diffusion ($Sh < 1$) or evaporation ($Sh > 1$) dominates the composition evolution. Power laws link the process duration, final solute coverage and the spatio-temporal evolution of the internal film composition to the control parameters and the properties of the initial solution. The analysis is relevant for casting real solutions, in particular for the deposition of specifically structured (sub)monolayers (“evaporation-induced self-assembly”). The quantitative validity of the analysis can be verified experimentally. Because the analysis provides palpable physical insight into the influence of the different process parameters, improvements regarding real (non-ideal) conditions can be implemented easily.

PACS numbers: 68.03.Fg, 47.57.eb, 47.85.mb, 82.70.-y

Introduction.—An excess amount of liquid deposited on a spinning, planar, wettable substrate forms a thinning film of uniform thickness h as the liquid flows outward (and is spun off) [1]. Evaporation of volatile film components adds to the film thinning (Fig. 1). The process of persistent deposition of non-volatile components on a spinning support is called “Spin Casting” or “Spin-Coating”. Coverage, structure, and other properties of the final deposit are strongly influenced by the processes occurring *during* film thinning. The nonvolatile components get continuously enriched, eventually exceeding saturation. The final deposit evolves from aggregation during film thinning in the presence of the solvent.

The application of spin casting is dominated by depositing polymer films with thicknesses up to tens of nanometers [2]. But increasingly it is also used to deposit structured (sub)monolayers, e.g., specific particle arrays (“evaporation-induced self-assembly”) [3–11]. Here we study the spin casting of ideal mixtures of a non-volatile solute and a volatile solvent to gain universal insights into the spatio-temporal composition evolution within the thinning film. For the first time the ideal spin cast equation is solved analytically. A universal cross-over behavior from hydrodynamic- to evaporation-dominated film thinning is revealed. The spatio-temporal composition evolution within the thinning film is analyzed with a diffusion-advection approach. General, palpable relations between the process parameters and the compositional evolution within the film are presented and the final solute coverage is calculated.

The insights are quantitatively valid for dilute solutions e.g., for a better understanding of evaporation-induced structuring of nano deposits. The quantitative revelation of the spatio-temporal composition evolution recommends spin casting of diluted solutions for

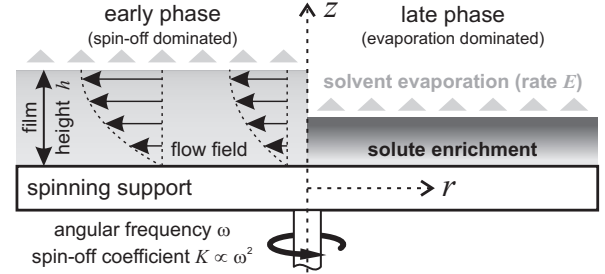


FIG. 1: Schematics of spin-casting with processes dominating early and late stages.

fundamental studies on nucleation and growth [8, 12]. Some results, e.g., the predicted solute coverage, are valid (semi-)quantitatively even for semi-dilute solutions. In addition, the findings improve the understanding of spin casting real polymer solutions despite their often individually distinctive, non-ideal rheological and evaporative behavior, because the physics behind the unveiled relations is comprehensive due to the largely analytical approach. Therefore our treatment also reveals excellent starting points for more detailed, system-specific analytical approaches of real systems [16].

I. Hydrodynamic-evaporative film thinning — The thinning of a Newtonian, volatile liquid film of thickness h on a rotating support is described by [13]:

$$dh/dt = -2K h^3 - E, \quad (1)$$

with spin-off coefficient $K = \omega^2/(3\nu)$, ω = rotational speed, ν = kinematic viscosity and E = evaporation rate. The fundamental form of Eq. 1,

$$d\xi/d\tau = -\xi^3 - 1, \quad (2)$$

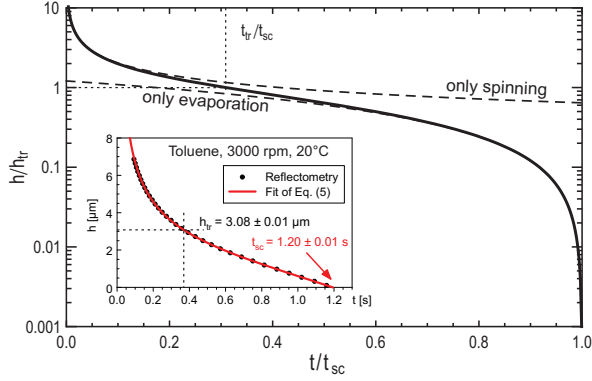


FIG. 2: Universal thinning curve $h/h_{tr} = f(t/t_{sc})$ (dashed lines: thinning due to spinning/evaporation only). Inset: Measured thinning curve in physical units for toluene and its fit according to the theory (Eq. 5).

is obtained by rescaling $\xi = h/h_{tr}$ and $\tau = t/t_{sc}^*$ i.e., by the system inherent “natural” scales:

$$h_{tr} = (E/2K)^{1/3}, \quad (3)$$

$$t_{sc}^* = (2E^2K)^{-1/3}. \quad (4)$$

h_{tr} is the “transition height” when evaporative and hydrodynamic thinning are equal. t_{sc}^* is the “reduced process duration” (Eq. 6).

Eq. 2 is nonlinear and inhomogeneous, but its inverse is of zeroth order, and can be integrated:

$$\tau(\xi) = \frac{\sqrt{3}}{6} \left\{ \pi + 2 \arctan \frac{1-2\xi}{\sqrt{3}} + \frac{1}{\sqrt{3}} \log \frac{1-\xi+\xi^2}{(1+\xi)^2} \right\}, \quad (5)$$

with integration constants so that $\tau = 0$ for $\xi \rightarrow \infty$. Because $\tau(\xi)$ is bijective, Eq. 5 also yields $\xi(\tau)$ respectively $h(t)$.

The duration of the whole process (starting at $h \rightarrow \infty$, ending at $h = 0$) is

$$t_{sc} = (2\pi/3^{3/2})(2E^2K)^{-1/3} = (2\pi/3^{3/2}) \cdot t_{sc}^*. \quad (6)$$

Fig. 2 shows the universal thinning curve (the inverse of Eq. 5) on scaled axes [17]. The findings agree with experimental results (see inset and [18]). The transition time, t_{tr} , at which h_{tr} is reached, is *universal* for all spin cast processes described by Eq. 1:

$$t_{tr} = \left((2\pi - \sqrt{3} \log 4) / (4\pi) \right) \cdot t_{sc} \approx 0.309 \cdot t_{sc}. \quad (7)$$

Hydrodynamic film thinning ($E = 0$, dotted) dominates $\approx 30\%$ of the spin cast time; $\approx 70\%$ is evaporation-dominated ($K = 0$, dashed).

II. Solute concentration evolution — During spin casting, non-volatile solute enriches at the free surface (where the solvent evaporates) and migrates into the film via diffusion. The spatio-temporal evolution of the solute concentration c is described by

$$\partial_t c = D \partial_z^2 c + K z^2 (3h - z) \partial_z c, \quad (8)$$

with boundary conditions [19]

$$D \partial_z c|_{z=h} = E c|_{z=h}, \quad \partial_z c|_{z=0} = 0. \quad (9)$$

The advective term in Eq. 8 is derived from the radial velocity field $u(r, z)$ of a Newtonian fluid rotating with its solid support (no slip), with a free surface at the top (no stress) [1]:

$$u(r, z) = 3K r z (h - z/2). \quad (10)$$

r and z are the radial respectively vertical coordinates. The radial volumetric flux ϕdz is

$$\phi dz = 2\pi r u(r, z) dz = 6\pi K r^2 z (h - z/2) dz. \quad (11)$$

With the continuity equation this yields the thinning-induced vertical motion of the horizontal stream lines:

$$dz/dt = -1/(2\pi r) \int_0^z \partial_r \phi dz' = -K z^2 (3h - z). \quad (12)$$

In order to solve Eq. 8, $h(t)$ is required but not known explicitly, only its inverse, $t(h)$ (Eq. 5). Since $h(t)$ respectively $\tau(\xi)$ are bijective, the time variable can be changed to ξ : $\partial_t c = d\tau/dt \cdot d\xi/d\tau \cdot \partial_\xi c = -(2E^2K)^{1/3}(\xi^3 + 1) \partial_\xi c$. Rescaling with $y = z/h$ ($y \in [0, 1]$, from substrate to surface) avoids the moving boundary. This leads to:

$$\partial_\xi c = -\frac{\partial_y^2 c}{Sh \xi^2 (\xi^3 + 1)} - \left\{ \frac{(\xi y)^2 (3 - y)}{2(\xi^3 + 1)} - \frac{y}{\xi} \right\} \partial_y c, \quad (13)$$

$$\partial_y c|_{y=1} = Sh \xi c|_{y=1}, \quad \partial_y c|_{y=0} = 0, \quad (14)$$

where the Sherwood number, Sh , parameterizes the ratio of evaporative to diffusive mass transport on the characteristic length scale of the system, h_{tr} :

$$Sh = E h_{tr}/D = E^{4/3} (2K)^{-1/3}/D. \quad (15)$$

By scaling c with the initial solute concentration c_0 the initial condition is $c|_{\xi \rightarrow \infty} = 1$. Thus the system is parametrized completely by Sh . Eq. 13 can be solved numerically with ξ as independent variable. Eq. 5 then provides τ as function of ξ i.e., finally, $c(t, z)$.

III. General aspects of the concentration evolution — Based on the solution of Eq. 13 the impact of Sh (i.e., of the individual system parameters K , E , and D) is now analyzed. Fig. 3 shows profiles of c during film thinning for Sh larger and smaller than 1 (i.e., convection dominating over diffusion and vice versa) and for film heights larger and smaller than h_{tr} , respectively. It reveals the competition between evaporative enrichment, spin-off, and diffusive dilution in both, spin-off and evaporation dominated regimes. In general, larger Sh means more pronounced gradients in c . If $h \gg h_{tr}$, solute enrichment occurs only locally near the free surface and $c \approx c_0$ near the substrate. If $h \ll h_{tr}$, c also increases

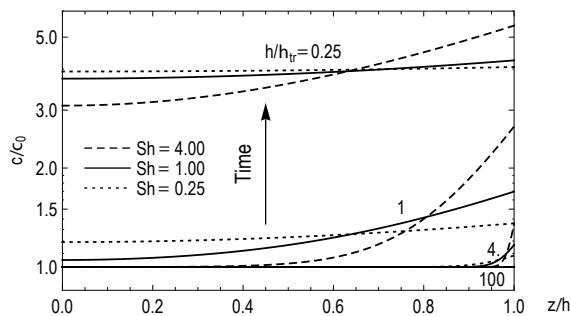


FIG. 3: Solute concentration profiles (resulting from Eq. 13) for three different Sherwood numbers Sh at three different moments respectively heights h/h_{tr} .

near the substrate. $Sh = 1$ and $h = h_{tr}$ mark the transition: The solute gradient just reaches the film/substrate interface and c just begins to increase globally.

Fig. 4 shows as function of h/h_{tr} : A) The total solute amount N per unit area A ($N/A = \int_0^h c dz$); B) c/c_0 at the surface respectively substrate/film interface; C) The difference between the surface and the substrate/film interface concentrations, $\Delta c/c_0$ i.e., the *relative* enrichment. Both, $h = h_{tr}$ and $Sh = 1$ mark transitions between distinctly different behaviors. I) For $h \gg h_{tr}$ spin-off dominates film thinning. Therefore, globally c/c_0 remains approximately constant and N/A decreases. Nevertheless, there is a surficial solute enrichment due to evaporation. But this $\Delta c/c_0$ only becomes substantial for $Sh > 1$. It has a maximum at $h = h_{peak}$ ($h_{peak} \approx h_{tr}$ for $Sh = \mathcal{O}(1)$). II) For $h \ll h_{tr}$, evaporation domi-

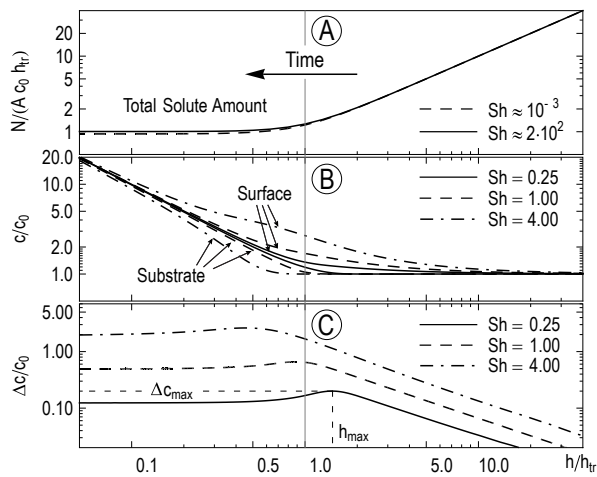


FIG. 4: For various Sherwood numbers Sh are shown as function of the reduced film thickness h/h_{tr} : A) Total solute amount N per per unit area A (scaled by $c_0 h_{tr}$); B) Concentrations c at the surface respectively film/substrate interface (scaled by c_0); C) Δc , the difference between the surface and the substrate/film interface concentrations, respectively (scaled by c_0).

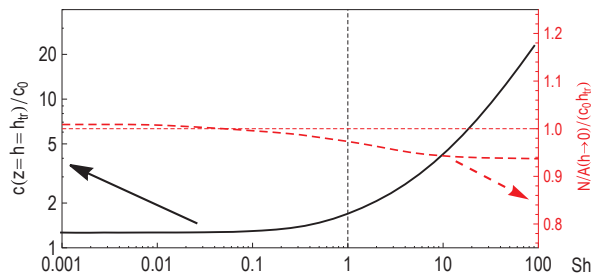


FIG. 5: Normalized final solute coverage, $N(h \rightarrow 0)/(A c_0 h_{tr})$ and c/c_0 at the film surface for $h = h_{tr}$ as function Sh .

ates. Solvent loss leads to increasing c/c_0 while N/A and $\Delta c/c_0$ remain constant (because spin-off becomes negligible). Remarkably, for $h < h_{tr}$, $N/(A c_0 h_{tr})$ remains approximately constant and independent from Sh whereas $\Delta c/c_0$ increases with increasing Sh .

Fig. 5 shows $c(z = h = h_{tr})/c_0$, the concentration at the free surface for $h = h_{tr}$, and $N(h \rightarrow 0)/(A c_0 h_{tr})$, the rescaled final coverage. Both are plotted as function of Sh . For $Sh \ll 1$ diffusion dominates and c is mostly homogeneous (Fig. 3). In this case $c_0 E t_{sc}$ is the total amount of solute that is *not* spun off with the solvent. Distributing this into a film with h_{tr} yields $c/c_0 = E t_{sc}/h_{tr} = 2\pi/3^{3/2} \approx 1.2$ (Fig. 5). The final solute coverage for $Sh < 1$ is (in agreement with [14])

$$\Gamma = N(h \rightarrow 0)/A \approx c_0 h_{tr} \approx 0.8 c_0 (K/E)^{-1/3}. \quad (16)$$

For $Sh \gg 1$ it is only $\approx 6\%$ lower.

IV. *Relative surficial enrichment maximum* — Fig. 6 shows $\Delta c_{max}/c_0$ and its spatio-temporal properties as function of Sh . Symbols denote the results from the numerical analysis. The solid lines show power laws for

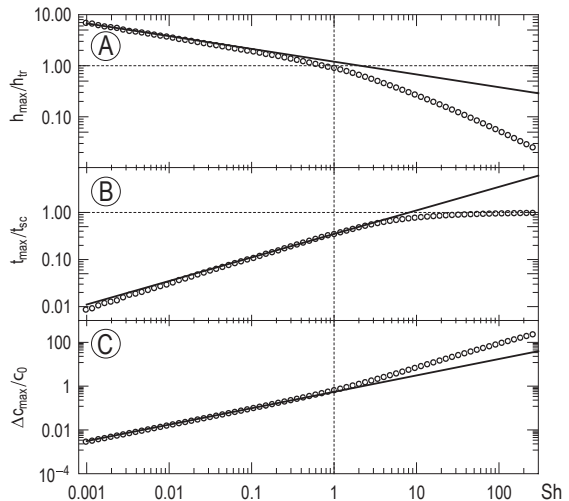


FIG. 6: $\Delta c_{max}/c_0$ as a function of Sh and related spatio-temporal properties ($h_{peak} = h|_{\Delta c_{max}}$ and $t_{peak} = t|_{\Delta c_{max}}$). The symbols indicate numerical results, the lines the underlying power laws for $Sh < 1$.

$Sh < 1$ which are rationalized by analyzing the underlying processes.

Panel A) shows h_{peak} rescaled by h_{tr} i.e., the film thickness at which $\Delta c = \Delta c_{max}$ as function of Sh . Δc_{max} emerges from the competition between evaporative enrichment, spin-off, and diffusional equilibration. Evaporation and spin-off dominate at opposite ranges of h . For large h , surficial spin-off efficiently suppresses enrichment: Δc_{max} requires $2Kh_{peak}^3 < E$ (from Eq. 1). However, for small h , diffusional equilibration is fast, so Δc_{max} requires $D/h_{peak} < E$. Optimizing both conditions simultaneously (E is linear and antagonistic in both cases, and therefore cancels out) reveals the same power law as numerics (which supplies the prefactor):

$$h_{peak} \approx (D/K)^{1/4} \approx 1.2 h_{tr} Sh^{-1/4}. \quad (17)$$

Panel B) shows the time t_{peak} rescaled by t_{sc} i.e., the time at which $\Delta c = \Delta c_{max}$. Before reaching h_{peak} , thinning is dominated by spin-off. Hence t_{peak} can be estimated by inserting h_{peak} into $h = (2Kt)^{-1/2}$ (the solution to Eq. 1 with $E = 0$):

$$t_{peak}/t_{sc} \approx 0.31 E^{2/3} K^{-1/6} D^{-1/2} \approx 0.35 \sqrt{Sh}. \quad (18)$$

Panel C presents $\Delta c_{max}/c_0$, reflecting the balance between evaporative enrichment and diffusive equilibration i.e., $Sh|_{h_{peak}} = E h_{peak}/D = Sh^{3/4}$. With Eq. 17 this means:

$$\Delta c_{max}/c_0 \approx 0.46 E K^{-1/4} D^{-3/4} \approx 0.55 Sh^{3/4}. \quad (19)$$

Discussion and Conclusions — Section I introduces the system-specific fundamental length and time scales (h_{tr} , t_{sc}^*) for the spin casting process of an ideal Newtonian volatile liquid. These reduce the general spin cast equation (Eq. 1) to its fundamental form. The equation is solved analytically for the first time revealing a universal film thinning behavior. The total spin coating time, t_{sc} is calculated (Eq. 6) as function of the process parameters (E , K , D). For any combination of these parameters, in the first 30% of the process time, thinning is governed by hydrodynamics. During the residual 70% of the time evaporative thinning dominates until complete drying.

Sections II through IV analyze the spin cast process assuming an ideal mixture of a volatile solvent and a non-volatile solute. It is found that the spatio-temporal evolution of the solute concentration within the thinning film is universally characterized by its Sherwood number, Sh , which reflects the competition between evaporative solute enrichment and diffusional dilution on the system-inherent fundamental length scale, h_{tr} . For $Sh < 1$ (diffusion dominates) the spatio-temporal occurrences of the solute concentration maxima are related to the process parameters via universal power laws (Eqs. 17, 18, and 19, see Fig. 6). These findings are rationalized semiquantitatively with the underlying physics. At last, the final

solute coverage Γ is calculated from the process parameters (Eq. 16).

To examine the relevance of our analysis for real cases, where E and K are not constant and depend on the solute concentration ($E = E(c)$, $K = K(\omega, \nu)$), we assume a typical solvent (e.g. toluene) with molar mass $M_s \approx 0.1$ kg/mol, density $\rho_s \approx 10^3$ kg/m³, $\nu = 6 \cdot 10^{-7}$ m²s⁻¹, and $E = 10^{-6}$ m/s [18]. We consider two examples: A) A typical polymer solution [2]; B) A nanoparticle solution for submonolayer deposition.

Case A): Polymer with $M_P = 100$ kg/mol, $\rho_P = 10^3$ kgm⁻³, and $c_{0,P} = 10$ kgm⁻³ (i.e., mole fractions $x_{0,P} = 10^{-6}$ and $x_{0,S} \approx 1$), $D_P = 10^{-11}$ m²s⁻¹ [15] and $K = 10^{11}$ m⁻²s⁻¹ (≈ 4000 rpm). This yields: $h_{tr} \approx 1.7 \cdot 10^{-6}$ m (Eq. 3), $Sh \approx 0.17$ (Eq. 15), $c_P(h_{tr})/c_{0,P} \approx 1.2$ (Figs. 3 and 5) and $\Gamma_P \approx 17 \cdot 10^{-6}$ kgm⁻² (Eq. 16) i.e., a final film thickness of ≈ 17 nm. This is reasonable [2].

Case B): Spheres with radius $r_{NP} = 36$ nm. $D_{NP} = 10^{-11}$ m²s⁻¹ (estimation: Stokes-Einstein) as in case A) and thus h_{tr} and Sh are identical to case A). A 50% monolayer coverage means $\Gamma_{NP} \approx 10^{14}$ m⁻² i.e., $c_{0,NP} \approx 5 \cdot 10^{-5}$ mol/m³ ($x_{0,NP} \approx 5 \cdot 10^{-9}$, $x_{0,S} \approx 1$) with Eq. 16.

In both cases c_0 is small ($x_{0,S} \ll 1$, $x_{0,NP} \ll 1$) i.e., the *initial* solution behaves approximately ideally. This means film thinning to h_{tr} will follow Eq. 1 with K and E remaining approximately constant because thinning is hydrodynamically dominated and the solute concentration barely changes. Hence Γ can be calculated with Eq. 16 because it is not affected by changes in K and E occurring *after* reaching h_{tr} .

For both examples $Sh < 1$. Therefore the data depicted for $Sh < 1$ in Figures 5 and 6 are relevant because h_{peak} , t_{peak} , and Δc_{max} occur at $h > h_{peak}$ when the solutions still behave approximately ideally. Accordingly, also Eqs. 17, 18 and 19 are applicable.

Of course, evaporative film thinning at $h < h_{peak}$ will eventually increase the solute concentration and thus change $E(c)$ and $K(\omega, \nu)$. However, in particular for "evaporation-structured" submonolayer particle array deposition, non-ideality will only become relevant for $h \ll h_{tr}$, when h is already in the range of r_{NP} , because typically $x_{0,NP} \ll 1$.

Our analysis provides valuable starting-points for improved approaches (other aspects) beyond the idealized continuum hydrodynamic-evaporative model. For instance, for low solubilities our analysis reveals where solute aggregation occurs first : A) at the top surface due to sufficiently high evaporative solute enrichment or B) globally homogeneous (or heterogeneously at the substrate) because diffusion keeps the (increasing) concentration approximately uniform.

Last not least, our analysis predicts a quantifiable behavior based on measurable parameters of the *initial* solution. In particular the predicted Γ and $h(t)$ [18] are easily measurable. Thus not only the validity of the approach can be evaluated. It is possible to specifically ad-

dress the influence of individual parameters of the multi-parameter spin casting process. For instance, parameters not related to mixing properties (e.g., temperature changes induced by evaporation) can be probed, because a sufficient reduction of c_0 will per definition render the solution behaving approximately “ideally”. All this proposes our approach as an excellent basis for incorporating specific (non)-linear properties of specific systems. Due to the predominantly analytic approach the basis still will be of general character and reveal palpable physical insights.

We thank Andreas Vetter and John Berg for scientific discussions, Helmuth Möhwald for scientific advice and general support. SK was funded by DFG Grant RI529/16-1, CMW by IGRTG 1524.

* Electronic address: stefan.karpitschka@mpikg.mpg.de

- [1] A. G. Emslie, F. T. Bonner, and L. G. Peck, *J. Appl. Phys.* **29**, 858 (1958).
- [2] K. Norrman, A. Ghanbari-Siahkali, and N. B. Larsen, *Annu. Rep. Prog. Chem. C* **101**, 174 (2005), in particular references 25 through 37 cited therein.
- [3] E. Rabani, D. R. Reichman, P. L. Geissler, and L. E. Brus, *Nature* **426**, 271 (2003).
- [4] T. P. Bigioni, X.-M. Lin, T. T. Nguyen, E. I. Corwin, T. A. Witten, and H. M. Jaeger, *Nat. Mater.* **5**, 265 (2006).
- [5] T. Hanrath, J. J. Choi, and D.-M. Smilgies, *ACS Nano* **3**, 2975 (2009).
- [6] A. T. Heitsch, R. N. Patel, B. W. Goodfellow, D.-M. Smilgies, and B. Korgel, *J. Phys. Chem. C* **114**, 1616 (2010).
- [7] E. Klecha, D. Ingert, and M. P. Pileni, *J. Phys. Chem. Lett.* **1**, 14427 (2010).
- [8] J. K. Berg, C. M. Weber, and H. Riegler, *Phys. Rev. Lett.* **105**, 076103 (2010).
- [9] A. C. Johnston-Peck, J. Wang, and J. B. Tracy, *Langmuir* **27**, 5040 (2011).
- [10] A. G. Marin, H. Gelderblom, D. Lohse, and J. H. Snoeijer, *Phys. Rev. Lett.* **107**, 085502 (2011).
- [11] M. A. Brookshier, C. C. Chusuei, and D. W. Goodman, *Langmuir* **15**, 2043 (1999).
- [12] H. Riegler and R. Köhler, *Nat. Phys.* **3**, 890 (2007).
- [13] D. Meyerhofer, *J. Appl. Phys.* **49**, 3993 (1978).
- [14] D. E. Bornside, R. A. Brown, P. W. Ackmann, J. R. F. Frank, A. A. Tryba, and F. T. Geyling, *J. Appl. Phys.* **73**, 585 (1993).
- [15] J. Rauch and W. Kohler, *Phys. Rev. Lett.* **88**, 185901 (2002).
- [16] For instance, the equations can rather easily be modified for concentration-dependent evaporation rates or viscosities
- [17] We assume the deposition of a liquid amount V^0 on the center of the substrate rotating with $\omega = const$ [1, 13]. V^0 is in large excess for forming a film hydrodynamically flattened to h_{tr} . Thus the process is experimentally well defined. V^0 barely affects t_{sc} due to the extremely fast initial decrease of h . Deposition prior to spinning, multi-drop depositions, etc., are not considered here.
- [18] See supplemental material at <http://link.aps.org/supplemental/...> for experimental thinning curves, a step-by-step derivation of Eq. 13, and details on the numerical methods.
- [19] Stefan condition at the free surface with evaporation, no diffusion through the substrate